

## Crystal Structure of Cesium-V

U. Schwarz

*Max-Planck-Institut für Festkörperforschung, Heisenbergstrasse 1, 70569 Stuttgart, Germany*

K. Takemura

*National Institute for Research in Inorganic Materials, Tsukuba, Ibaraki 305-0044, Japan*

M. Hanfland

*European Synchrotron Radiation Facility, BP220, F-38043 Grenoble, France*

K. Syassen

*Max-Planck-Institut für Festkörperforschung, Heisenbergstrasse 1, 70569 Stuttgart, Germany*

(Received 19 June 1998)

The crystal structure of the high-pressure phase cesium-V was investigated using monochromatic synchrotron x-ray diffraction. Full profile refinements of powder diffraction data resulted in a solution with space group  $Cmca$  and 16 atoms in the orthorhombic unit cell. The Cs-V structure can be viewed as a distorted fcc structure. Atoms occupy two different Wyckoff positions with 10-fold and 11-fold coordination, respectively. This new structure type is considered a possible candidate for high-pressure phases of other elemental metals. [S0031-9007(98)07211-1]

PACS numbers: 61.50.Ks, 61.66.Bi, 62.50.+p, 64.70.Kb

Cesium metal exhibits an unusual sequence of phase transitions under pressure [1–5]. Near 4.2 GPa, the high-pressure fcc phase (Cs-II) undergoes a first-order *isostructural* transition [3] to the collapsed fcc phase Cs-III (volume change  $-9\%$ ). At 4.4 GPa there follows a transition to the tetragonal Cs-IV phase, where, contrary to the pressure-coordination rule, the number of atoms in the first coordination shell is *reduced* from twelve to eight [6]. The structure of Cs-IV is related to the  $ThSi_2$ -type structure [7]. In the vicinity of the Cs-IV to Cs-V transition near 12 GPa, cesium becomes superconducting [8]; i.e., it is the only known superconducting alkali metal. At this pressure, cesium is compressed to 26% of its normal volume. The phase Cs-V persists up to 72 GPa, where another structural transition to the nearly close-packed phase Cs-VI takes place [9].

The anomalously large compressibility of cesium below 10 GPa [10], its structural behavior [3,6,9], and experimental observations concerning the melting curve [2,5], electrical transport [3,4,8], and optical properties [11] have been interpreted in terms of an electronic transition, where the  $6s$  valence electrons undergo a transfer to more localized  $5d$ -like states at high pressure. Detailed electronic structure calculations have been performed which support this picture (see, e.g., Refs. [12–14]). In particular, near the Cs-IV to Cs-V transition the calculated  $d$  occupation number has reached a value of 0.8 [13]. Thus, Cs-V has the unusual property of being a monovalent metal with essentially one outer  $d$  valence electron. Crystal structure information is essential for understanding the electronic properties and the chemical bonding of Cs-V as well as possible consequences for the high-pressure behavior of neighboring  $d$ -electron elements.

In this Letter we report a structure determination of Cs-V based on high-resolution angle-dispersive powder x-ray diffractometry. We assign an orthorhombic structure with 16 atoms per unit cell ( $oC16$  in Pearson notation). In this structure Cs atoms occupy two crystallographically inequivalent positions characterized by 10-fold and 11-fold coordination. This is the first observation of the  $oC16$  structure for an elemental metal.

The crystal structure of Cs-V was previously investigated by laboratory x-ray diffraction [15]. Three structure candidates were proposed. A unique structure assignment was not possible mainly due to insufficient resolution. In a more recent energy-dispersive synchrotron x-ray diffraction study of Cs-V [16], all three of the proposed structures were ruled out, but no alternative structure model was presented. In the present experiment we have taken advantage of the high angular resolution and reliable intensity measurements attainable in monochromatic (angle-dispersive) high-pressure powder diffraction at the European Synchrotron Radiation Facility (ESRF). These features turned out to be essential for the unambiguous structure solution reported here.

The diffraction experiments were performed at the undulator beam line ID9 of the ESRF using a diamond anvil high-pressure cell (DAC) with beryllium backing plates and an image plate detection system at about 45 cm distance from the sample. Wavelength selection, focusing, and removing of higher-order harmonics were achieved by a combination of a bent Si mirror and a Si(111) focusing Laue monochromator. The x-ray beam (wavelength 0.45798 or 0.44618 Å) was collimated to a nominal diameter of 30  $\mu\text{m}$ . In order to improve powder averaging, the DAC was oscillated by  $\pm 3^\circ$ . The scanned

two-dimensional diffraction patterns were corrected for tilt and scanner distortions and converted to intensity vs  $2\Theta$  data using the FIT2D software [17]. Determination of peak positions, indexing, structure solution, and refinements were performed using the CSD program [18].

Since Cs metal easily reacts with oxygen and moisture, special care was taken in the sample preparation. Cesium was obtained by reaction of dried CsCl (+99.5%) with vacuum-heated Ca (+98.5%) and then purified by twofold distillation [19]. Inside a glove box with oxygen-free dry argon atmosphere, a drop of liquid cesium (melting point  $29^\circ\text{C}$ ) was filled into the gasket hole ( $180\ \mu\text{m}$  diameter) of the DAC. A ruby chip served as an optical pressure sensor [20]. No pressure medium was used in order to avoid any contamination of the sample. After loading into the DAC, the color of the cesium remained silver metallic. Color changes at pressure-induced phase transitions could be detected by microscope observation. Some diffraction data were taken after thermal annealing at  $450\ \text{K}$  for 8 h. In this way the width of low-angle diffraction peaks was reduced to less than  $0.04^\circ$ .

Powder patterns of cesium measured at pressures between 7.4 and 11 GPa proved that the samples were single phase Cs-IV. No extra lines due to the formation of oxides were detected. Also, no evidence was seen which would allow for Pauling's interpretation [21] of earlier diffraction results [6] for Cs-IV. At pressures at about 11.0(5) GPa, the appearance of new diffraction peaks indicated the onset of the structural transformation to Cs-V which was completed near 12.0(5) GPa for increasing pressure. The transition was fully reversible with a hysteresis width of 2 GPa. The diffraction diagrams of Cs-V were slightly spotty. However, the integration of full Debye-Scherrer

rings led to reliable intensities. Also, reproducible peak intensities were observed in different runs. A representative diffraction diagram of Cs-V is shown in Fig. 1. The insets in this figure demonstrate specific aspects of the data, e.g., the excellent angular resolution and the detection of very weak low-angle reflections.

On the basis of an orthorhombic unit cell, 93 lines observed up to a maximum scattering angle of  $30^\circ$  could be indexed. Systematic extinctions indicated *Cmca* (No. 64) or *C2cb* (No. 41, nonstandard setting of *Aba2*) as possible space groups (SG). The crystal structure was solved in the centric SG *Cmca* using direct methods. For this solution, atoms occupy the Wyckoff positions  $8f$  and  $8d$ . Atoms in these positions are denoted as Cs-1 and Cs-2, respectively. The resulting positional parameters served as starting values in the full profile refinements. In the final fit of the diffraction profile preferred orientation was taken into account. The line in Fig. 1 marked *R* corresponds to the difference between experimental profile and refinement. Obviously, the structural model gives an excellent description of the experimental pattern. Results of refinements at selected pressures are listed in Table I. All refinements are of similar quality, as indicated by the residuals  $R_I$  [22]. The volume difference between Cs-IV and Cs-V amounts to  $\Delta V/V = -9.3\%$  at 12 GPa.

The crystal structure of Cs-V is depicted in Fig. 2. A characteristic feature are layers of corner-sharing octahedral atom groups with interatomic distances which differ by less than 3%. Each Cs-1 atom in the equatorial plane of the octahedra has a fifth contact to a Cs-1 atom in a neighboring group. This is actually the shortest atom contact. The resulting five-coordinated nets formed by the Cs-1 atoms (see also Fig. 3) are common for intermetallic

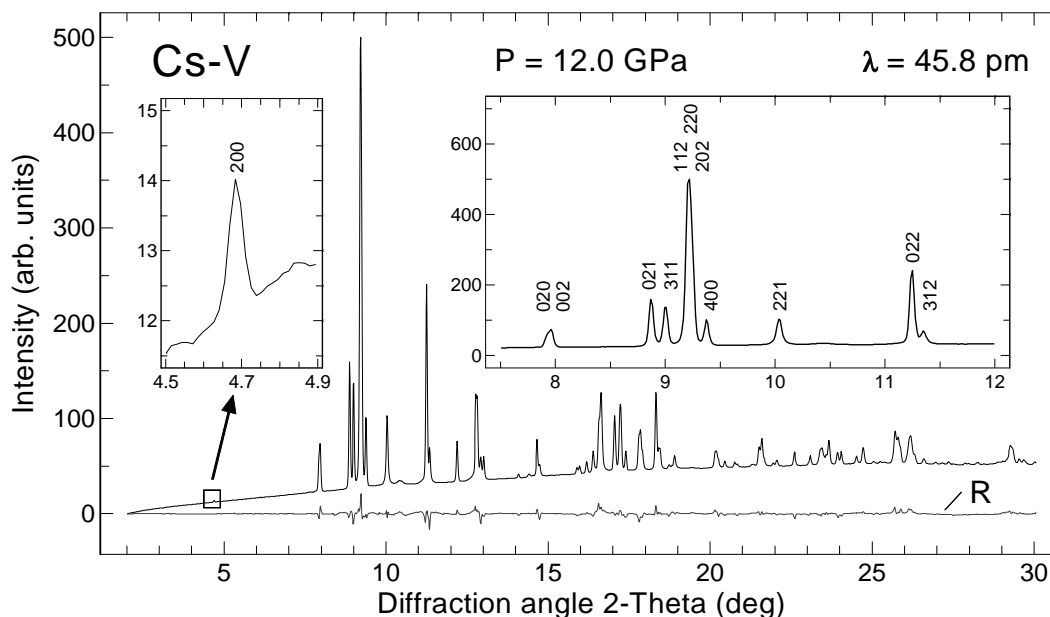


FIG. 1. Angle-dispersive synchrotron x-ray diffraction pattern of Cs-V at 12 GPa. The insets show expanded portions of the data. The curve marked *R* represents the difference between data and the refined profile for the *Cmca* structure.

TABLE I. Results of structure refinements for Cs-V (SG  $Cmca$ ,  $Z = 16$ ) at selected pressures. Positional parameters  $x$ ,  $y$ , and  $z$  refer to the corresponding axes in the  $Cmca$  space group. The coordinates for Cs-1 (8*f*) and Cs-2 (8*d*) are (0,  $y$ ,  $z$ ) and ( $x$ , 0, 0), respectively. Other coordinates follow from space group symmetry. The distances  $d$  are given for atoms in the first coordination sphere. Relative experimental errors for lattice parameters are  $3 \times 10^{-4}$ , absolute uncertainties for positional parameters are about  $2 \times 10^{-3}$ .

P (GPa)	12.0 <sup>a</sup>	19.6	25.8
$a$ (Å)	11.205	10.879	10.641
$b$ (Å)	6.626	6.443	6.278
$c$ (Å)	6.595	6.389	6.249
$a/c$	1.699	1.696	1.699
$b/c$	1.005(1)	1.008(2)	1.005(1)
$y$ (Cs-1)	0.1729	0.1781	0.188
$z$ (Cs-1)	0.327	0.328	0.328
$x$ (Cs-2)	0.2161	0.2118	0.2173
$R_I$ (%)	9	5	16
$V_{\text{atom}}$ (Å <sup>3</sup> )	30.60	27.98	26.09
$d_{\text{short}}$ (Å)	3.237	3.180	3.176
$d_{\text{long}}$ (Å)	3.612	3.474	3.402
$d_{\text{other}}$ (Å)	3.404	3.322	3.213
	to 3.464	to 3.371	to 3.314

<sup>a</sup>Measured for decreasing pressure.

compounds [23], e.g.,  $\text{CuAl}_2$ . Layers of octahedra are stacked on top of each other in an alternating fashion. The additional bonds thus formed between Cs-1 and Cs-2 atoms (thick open lines in Fig. 2) are about 5% longer compared to the average distance within the polyhedra. The Cs-1 and Cs-2 atoms have 11-fold and 10-fold coordination, respectively.

Taking the experimental errors into account, there is no pressure dependence of axial ratios (see Table I). This suggests that the structure represents a relatively rigid atomic arrangement. The only clear pressure effect is a reduction of the ratio  $d_{\text{long}}/d_{\text{short}}$  of the longest to the shortest atom distance with increasing pressure.

The local coordination in the Cs-V structure differs from that reported in an earlier diffraction study [15]. However, the unit cell of the Cs-V structure is just twice as large compared to the tetragonal structure proposed previously. Thus, pressure-volume data derived on the basis of the earlier tetragonal structure assignment are approximately correct.

The Cs-V structure can be described as a distorted fcc or body-centered tetragonal (bct) structure. This is illustrated in Fig. 3, which shows views of the Cs-V structure along the  $a$  axis and of the fcc (bct) structure along the  $[001]$  direction. Starting from a fcc lattice, one arrives at the Cs-V structure by rotating six-atom clusters around the centers of every second octahedral void within a  $(001)_{\text{fcc}}$  plane (rotation axis parallel to  $[001]_{\text{fcc}}$ ). Neglecting bond bending forces, the maximum possible rotation is determined by the distance of atoms in the newly formed contact. The result is a  $\sqrt{2} \times \sqrt{2}$  superstructure relative to the  $(001)_{\text{fcc}}$

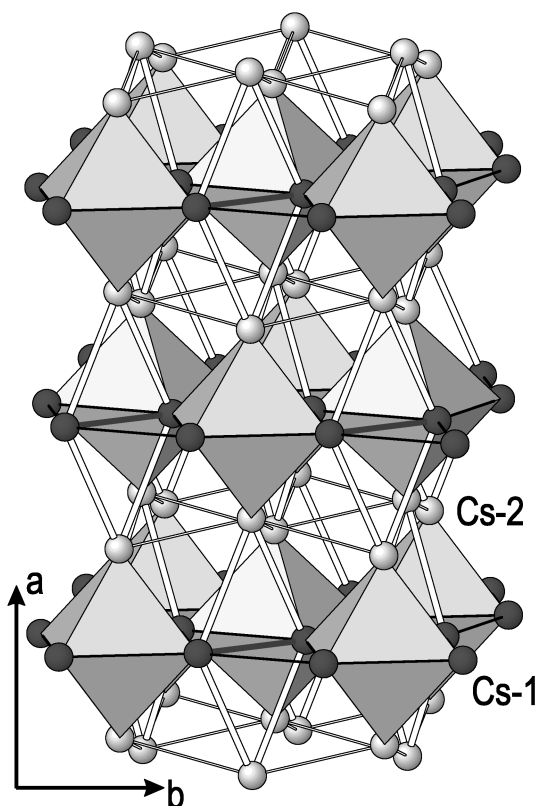


FIG. 2. Perspective view of the  $Cmca$  crystal structure of Cs-V. Atoms occupy two different Wyckoff positions. The thick solid and open lines between atoms indicate the shortest and longest bond lengths, respectively, in the first coordination sphere. The octahedra mark nearly close-packed units. Note that there are no central atoms inside the octahedra.

plane. The senses of rotation alternate in subsequent layers of octahedra of the fcc lattice. The unit cell length is thus doubled along  $[001]_{\text{fcc}}$ . The rotation reduces the area covered by a projection onto the  $(001)_{\text{fcc}}/(100)_{\text{ortho}}$  plane, if one assumes a constant bond length within octahedral groups. If the five Cs-1–Cs-1 bonds in the corresponding

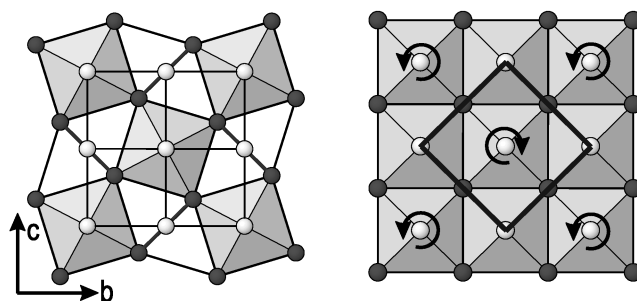


FIG. 3. Left: View of the Cs-V structure along the  $a$  axis emphasizing the five- and four-coordinated two-dimensional nets. Thick lines connecting pairs of Cs-1 atoms (dark color) mark the shortest contacts. Right: View of a fcc (bct) structure along the  $[001]$  direction. The fcc unit cell is marked by thick lines. Arrows indicate the rotations of octahedra which, in combination with atomic displacements, lead from the fcc to the Cs-V structure (see text).

(100)<sub>ortho</sub> plane were of equal lengths, a volume conserving process would require an expansion along [100]<sub>ortho</sub> corresponding to an  $a/c$  ratio of 1.52 for the orthorhombic cell. In the observed structure the Cs-2 atom layers are corrugated and the  $a/c$  ratio increases to about 1.7.

While Cs-IV clearly has an open structure which can be interpreted in terms of a local bonding picture [7,14], Cs-V approaches a dense packing of atoms. Thus, the driving force for a distortion away from fcc is not easily identified, in particular since, relative to fcc, a superstructure is formed in all three directions. Correspondingly, the formation of an enhanced density of states below the Fermi level, which would stabilize the Cs-V structure relative to fcc, involves several folded band states. On the other hand, two features of the Cs-V structure stand out clearly, the octahedral groups and the short Cs-1–Cs-1 contacts. If the formation of these contacts involves formation of a covalent bond, some energy gain is expected from a bonding-antibonding splitting. Within a local bonding picture, one could envision another possible stabilizing element of the Cs-V structure, namely, an electron density distribution which favors the formation of octahedral groups.

We briefly mention that the isostructural fcc-fcc transition of cesium [3] was not confirmed in the present study. Because of recrystallization, the diffraction patterns measured in the stability range of Cs-III (4.2 to 4.4 GPa) consisted of spots originating from single crystal regions. Two  $d$  spacings of about 7.5 and 35 Å were evident in the diffraction patterns, indicating the formation of a phase with a large-period supercell. More systematic studies of the structural behavior of cesium in this very interesting pressure range are underway.

In conclusion, we have determined the crystal structure of Cs-V using high-resolution synchrotron x-ray diffraction. The orthorhombic structure with space group  $Cmca$  and 16 atoms per unit cell (8 atoms in a primitive cell) is closely related to the fcc structure. A simple distortion of fcc results in the formation of a unit cell 4 times larger than that of the fcc lattice. A characteristic feature of the Cs-V structure is that Cs atoms occupy two crystallographically inequivalent sites with coordination numbers of 10 and 11. At this point, the Cs-V structure is unique among elemental solids. We suggest, however, to test this structure as a possible candidate for unsolved high-pressure phases, among them distorted fcc phases in lanthanides [24] and the phase Rb-VI [25].

We thank U. Oelke, W. Dieterich, and U. Engelhardt for technical assistance, and F. Koegel for the preparation of the sample. During this work, we have enjoyed helpful discussions with Yu. Grin.

- [1] P. W. Bridgman, Proc. Am. Acad. Arts Sci. **76**, 55 (1948).
- [2] G. C. Kennedy, A. Jayaraman, and R. C. Newton, Phys. Rev. **126**, 1363 (1962).
- [3] H. T. Hall, L. Merrill, and J. D. Barnett, Science **146**, 1297 (1964).
- [4] R. A. Stager and H. G. Drickamer, Phys. Rev. Lett. **12**, 19 (1964).
- [5] A. Jayaraman, R. C. Newton, and J. M. McDonough, Phys. Rev. **159**, 527 (1967).
- [6] K. Takemura, S. Minomura, and O. Shimomura, Phys. Rev. Lett. **49**, 1772 (1982).
- [7] H. G. von Schnering and R. Nesper, Angew. Chem. **99**, 1097 (1987); Angew. Chem. Int. Ed. Engl. **26**, 1059 (1987).
- [8] J. Wittig, Phys. Rev. Lett. **24**, 812 (1970); J. Wittig, in *Superconductivity in  $d$ - and  $f$ -band Metals*, edited by W. Buckel and W. Weber (Kernforschungszentrum Karlsruhe, Karlsruhe, 1982).
- [9] K. Takemura, O. Shimomura, and H. Fujihisa, Phys. Rev. Lett. **66**, 2014 (1991).
- [10] D. B. McWhan, G. Parisot, and D. Bloch, J. Phys. F **4**, 169 (1974).
- [11] H. Tups, K. Takemura, and K. Syassen, Phys. Rev. Lett. **49**, 1776 (1982).
- [12] S. G. Louie and M. L. Cohen, Phys. Rev. B **10**, 3237 (1974).
- [13] A. K. McMahan, Phys. Rev. B **17**, 1521 (1978); D. Gloetzel and A. K. McMahan, Phys. Rev. B **20**, 3210 (1979); A. K. McMahan, Phys. Rev. B **29**, 5982 (1984).
- [14] O. K. Andersen, N. E. Christensen, S. Pawłowska, and O. Jepsen (unpublished).
- [15] K. Takemura and K. Syassen, Phys. Rev. B **32**, 2213 (1985).
- [16] J. V. Badding, H. K. Mao, and R. J. Hemley, Solid State Commun. **77**, 801 (1991).
- [17] A. Hammersley, computer program FIT2D, ESRF Grenoble, 1998.
- [18] L. G. Akselrud, Yu. Grin, V. K. Pecharsky, P. Yu. Zavaliy, and V. S. Fundamenskiy, computer program CSD 4.10, STOE & Cie, Darmstadt, 1992.
- [19] A. Simon, Z. Anorg. Allg. Chem. **395**, 301 (1973).
- [20] G. J. Piermarini, S. Block, J. D. Barnett, and R. A. Forman, J. Appl. Phys. **46**, 2774 (1975); H. K. Mao, J. Xu, and P. M. Bell, J. Geophys. Res. **91**, 4673 (1986).
- [21] L. Pauling, Proc. Natl. Acad. Sci. USA **86**, 1431 (1989).
- [22] Residuals are for peak intensities only, not including background intensity. For comparison, refinements of diffraction data for Cs-IV (SG  $I4_1/amd$ , a parameter-free structure) yielded  $R_I$  values of typically 10%.
- [23] B. G. Hyde and S. Andersson, *Inorganic Crystal Structures* (Wiley, New York, 1989).
- [24] W. B. Holzapfel, J. Alloys Compd. **223**, 170 (1995).
- [25] M. Winzenick, V. Vijayakumar, and W. B. Holzapfel, Phys. Rev. B **50**, 12381 (1994).